

Supporting Information

1. Sources of variance in S_{vO_2} -TRUST measurement

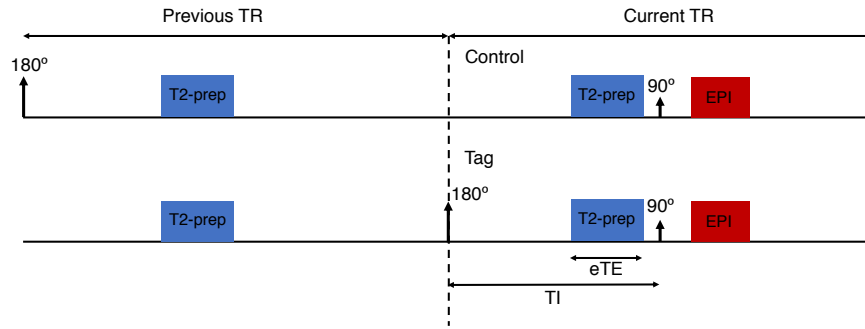
1.1 Underestimation of T2 due to short TR

In the original TRUST sequence proposed by Lu and Ge (1), the longitudinal magnetization of blood spins is assumed to fully recover every TR. The final difference signal is a mono-exponential decay w.r.t. the effective echo time (eTE):

$$M_z = 2M_0 e^{-eTE \cdot (R_{2b} - R_{1b})} e^{-TI \cdot R_{1b}} \quad [1]$$

where R_{1b} and R_{2b} are the relaxation parameters of venous blood.

However, use of short TR (e.g. TR = 3000 ms in this study) can cause T2 underestimation. This bias has been described by Xu et al. (2). Here, we explicitly present the signal function considering spin history and describe an approach to retrospectively correct the T2 underestimation error.



Supporting Information Figure S1. Pulse sequences experienced by blood spins in two consecutive TRs. The TRUST sequence acquires control and labeled images in an interleaved manner. Blood spins are assumed to locate in the labeling slab during the previous TR and stay in the imaging slice during the current TR. (top) Illustration of control imaging, in which blood spins have experienced an inversion RF pulse and a T2-preparation module in the previous TR. (bottom) Illustration of tag imaging, in which blood spins have only experienced a T2-preparation module in the previous TR.

The TRUST sequence used in this study acquired control and labeled images in an interleaved manner. If the current TR is for control imaging, then blood spins will have experienced an inversion RF pulse and a T2-preparation composition pulse in the previous TR without adequate time for full T1 recovery (Supporting Information Figure S1 top). Accounting such spin history, signal in the control image is:

$$M_{z,\text{control}} = M_0 \left[(1 - 2e^{-(TI-eTE) \cdot R_{1b}}) e^{-eTE \cdot R_{2b}} e^{-(TR-eTE) \cdot R_{1b}} + 1 - e^{-(TR-eTE) \cdot R_{1b}} \right] e^{-eTE \cdot R_{2b}} \quad [2]$$

If the current TR is for tag imaging, then blood spins will have experienced a T2-preparation pulse in the previous TR (Supporting Information Figure S1 bottom). In this case, signal in the tag image is:

$$M_{z,\text{tag}} = M_0 \left[-e^{-eTE \cdot R_{2b}} e^{-(TR-eTE) \cdot R_{1b}} + e^{-(TR-eTE) \cdot R_{1b}} + 1 - 2e^{-(TI-eTE) \cdot R_{1b}} \right] e^{-eTE \cdot R_{2b}} \quad [3]$$

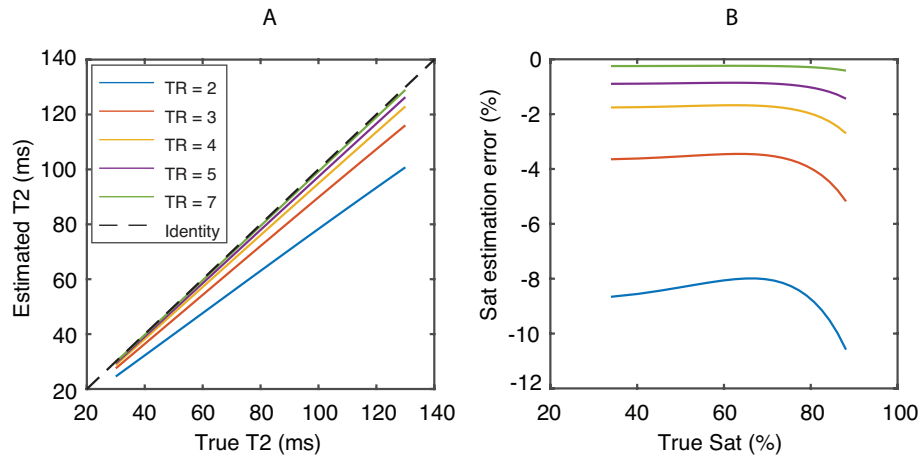
The difference signal is:

$$M_{z,\text{diff}} = M_0 \left[e^{-eTE \cdot (2R_{2b} - R_{1b})} (e^{-TR \cdot R_{1b}} - e^{-(TR+TI-eTE) \cdot R_{1b}}) + e^{-eTE \cdot (R_{2b} - R_{1b})} (e^{-TI \cdot R_{1b}} - e^{-TR \cdot R_{1b}}) \right] \quad [4]$$

Signals at eTE = 0, 40, 80, 160 ms were simulated based on Eq. [4], using the following parameters: TR = 2~7 s, T1 = 1022 ms, T1 of blood = 1620 ms, T2 of blood = 20~130 ms. Underestimation of T2 is demonstrated by performing mono-exponential fitting to the simulated signals (Supporting Information Figure S2A). In the case of TR = 3 s, a one-to-one relation between estimated T2 and true T2 is obtained by linear regression:

$$T2_{\text{cor}} = 1.1 \times T2_{\text{est}} - 1.2 \quad [5]$$

where $T2_{\text{est}}$ and $T2_{\text{cor}}$ are the estimated and corrected T2 measurement (ms). Eq. [5] was used to correct the underestimation of T2 due to short TR in the present study. Assuming Hct = 0.42, T2 underestimation can be converted into saturation underestimation using the bovine blood calibration model. Saturation underestimation is approximately constant over a range of true saturation from 30% to 80% (Supporting Information Figure S2B).

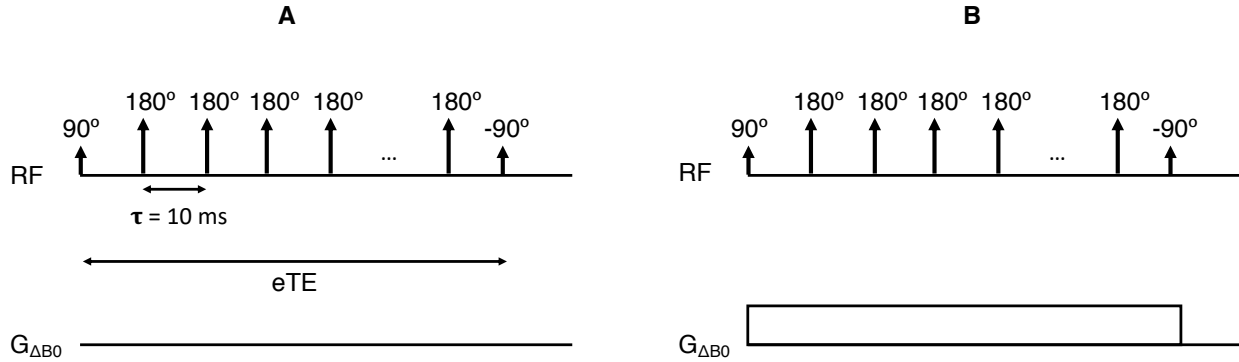


Supporting Information Figure S2. Simulation of T2 underestimation caused by short TR. A. T2 estimated from mono-exponential fitting is plotted against the true T2 (ms) in cases of different TRs (s). B. Assuming Hct = 0.42, T2 underestimation is converted into saturation underestimation using the bovine blood calibration model.

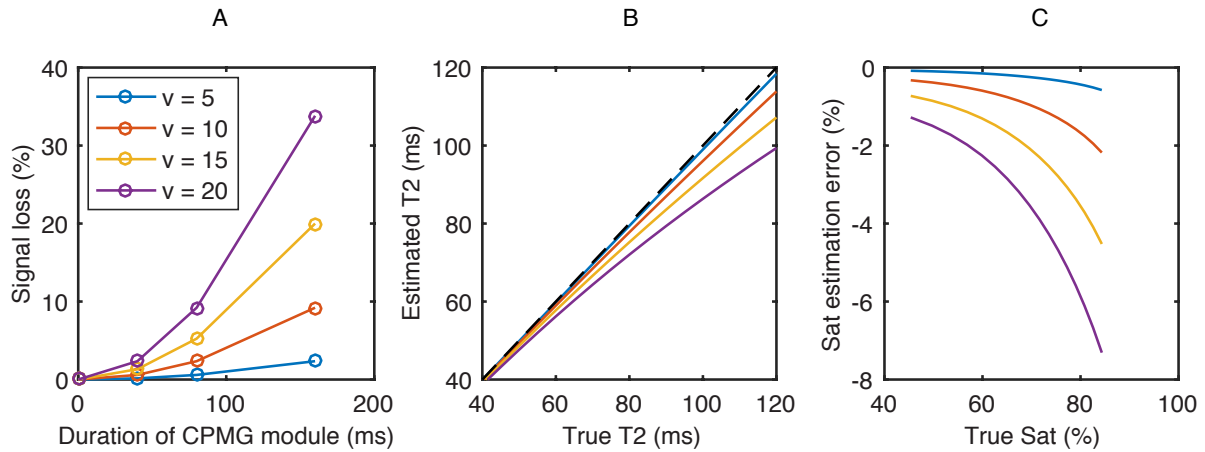
1.2 Underestimation of T2 due to intravoxel dephasing

Ideally, the T2-preparation module in TRUST sequence induces signal decay that depends on the T2 relaxation of venous blood (Supporting Information Figure S3A). However, B_0 field inhomogeneity can cause additional signal loss for flowing spins. Brown et al. (3) presented a mathematical description of intravoxel dephasing due to flow and accompanying gradient fields. Assuming a laminar flow model, the ratio of signal loss is $(1 - \text{sinc}(\phi))$, where ϕ is the phase dispersion within the voxel. We simulated such intravoxel dephasing effect by approximating the B_0 field variation in the brain as a gradient field of 1500 Hz/m (Supporting Information Figure S3B). For spins flowing at a rate of 20 cm/s, intra-voxel phase dispersion were 0.12π , 0.24π and 0.48π at eTE of 40 ms, 80 ms and 160 ms, which correspond to signal loss ratio of 2.3%, 9.2%, and 33.8% respectively (Supporting Information Figure S4A). Such signal loss adds on top of

the T2 decay, thus causing T2 underestimation. Using the bovine blood model and assuming true saturation of 60% and Hct of 0.42, the resultant saturation underestimation was 2% for spin velocity of 20 cm/s and ignorable for spin velocity of 5 cm/s (Supporting Information Figure S4C). Saturation estimation error increased with spin velocity (cm/s) and the true saturation.



Supporting Information Figure S3. Comparison of the T2-preparation module without (A) and with (B) B_0 field inhomogeneity (approximated as a gradient field, $G_{\Delta B_0}$).

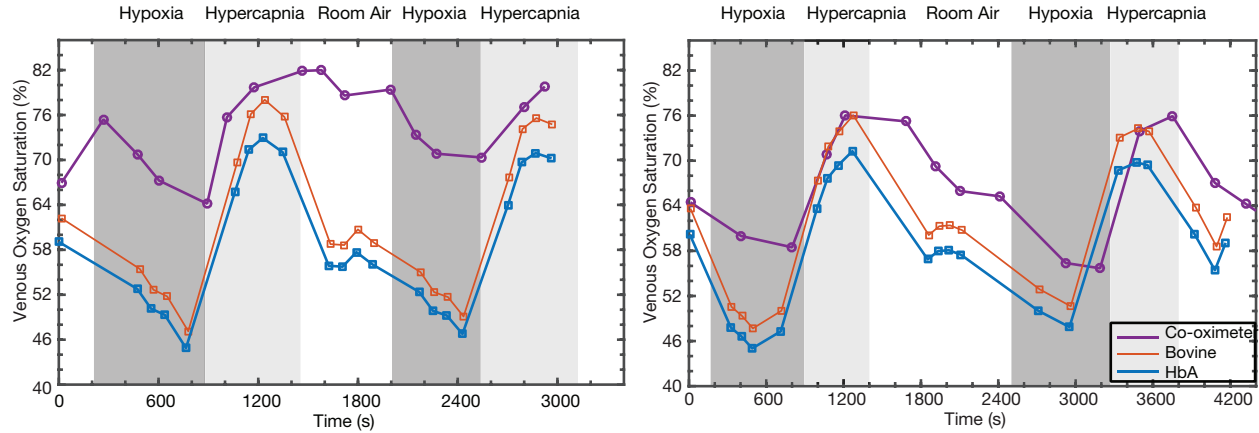


Supporting Information Figure S4. Effect of intra-voxel dephasing on T2 estimation, assuming the B_0 field variation as a gradient field of 1500 Hz/m. A. Signal loss ratio (%) depends on both the spin velocity (cm/s) and the duration of the CPMG T2-prep module (ms). B. T2 estimated from single-exponential fitting is plotted against the true T2 (ms) in cases of different spin velocities. C. Using the bovine blood model and assuming Hct of 0.42, simulated saturation error increases with spin velocity (cm/s) and the true saturation.

1.3 Choice of calibration model

Critical to TRUST is the empirically derived calibration model that converts T2 of blood into oxygen saturation. The most widely used T2 calibration model at 3 tesla was proposed by Lu et al. (4) in experiments using bovine blood. Recently, Bush et al. (5) proposed another T2 calibration model based on healthy human blood (“human HbA model”). To investigate whether the choice of T2 calibration model contributes to the systematic bias we observed between S_vO_2 -TRUST and co-oximeter reference, we used

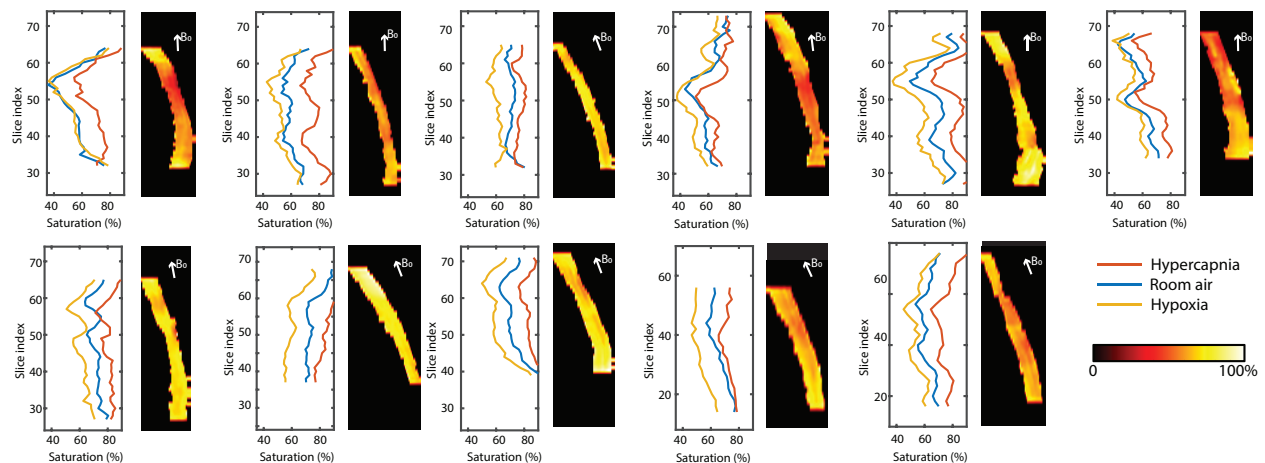
both the bovine blood and human HbA models to obtain intravascular S_vO_2 measurements. From Supporting Information Figure S5, it can be seen that the bias between TRUST and co-oximeter reference did not vary significantly with the choice of T2 calibration model.



Supporting Information Figure S5. Time-course plots of S_vO_2 measurements using co-oximeter (purple), TRUST with bovine blood model (orange) and TRUST with HbA model (blue) in two subjects who underwent jugular catheterization.

2. Variance in S_vO_2 -SBO measurement

The acquisition of a 3D ΔB_0 field map allowed us to investigate the variance of S_vO_2 measurement using conventional 2D SBO acquisition and processing. For each dataset, all axial slices where the SSS tilt angle was within 30° with respect to the main B_0 field were identified. In each of these viable slices, ΔB_0 shift inside the cross-section of SSS was converted to venous blood susceptibility using the 2D processing approach proposed by Jain et al. (6). Variation range was calculated as the difference between the maximum and minimum S_vO_2 measurements across all viable slices. We observed large variation of S_vO_2 measurements along the slice direction in every subject (Supporting Information Figure S6). On average, the range of variation was 22% in absolute saturation points.



Supporting Information Figure S6. Large variation of S_vO_2 -SBO measurement along the head-feet direction. Each subplot represents one subject. The 2D S_vO_2 -SBO measurement (horizontal axis) is plotted as a function of slice index (vertical axis). Measurements under hypercapnia, hypoxia and room air are represented as red, yellow and blue lines. Susceptibility of SSS measured under room air condition is converted to S_vO_2 values and plotted in sagittal view aligning with the vertical axis of the S_vO_2 plot. Orientation of the main B_0 field is labeled.

3. S_vO_2 -TRUST measurement in straight sinus

S_vO_2 of the straight sinus (SS) was also measured using TRUST in the 11 subjects scanned without jugular catheterization. The acquisition was performed immediately after the TRUST measurement of the SSS under each oxygenation condition. The sequence was the same except that the imaging slice was placed cutting across the SS. S_vO_2 -TRUST of SS was systematically higher than that of SSS under all three oxygenation conditions (hypoxia $5.7 \pm 5.1\%$, $p = 0.02$, room air $4.5 \pm 3.0\%$, $p = 0.08$, and hypercapnia $2.3 \pm 3.0\%$, $p = 0.37$).

References:

1. Lu H, Ge Y. Quantitative evaluation of oxygenation in venous vessels using T2-Relaxation-Under-Spin-Tagging MRI. *Magn. Reson. Med.* 2008;60:357–363 doi: 10.1002/mrm.21627.
2. Xu F, Uh J, Liu P, Lu H. On improving the speed and reliability of T2-relaxation-under-spin-tagging (TRUST) MRI. *Magn. Reson. Med.* 2012;68:198–204 doi: 10.1002/mrm.23207.
3. Brown RW, Haacke EM, Cheng YC, Thompson MR, Venkatesan R. *Magnetic resonance imaging: physical principles and sequence design*. New York: John Wiley & Sons; 1999. 673-675 p.
4. Lu H, Xu F, Grgac K, Liu P, Qin Q, van Zijl P. Calibration and validation of TRUST MRI for the estimation of cerebral blood oxygenation. *Magn. Reson. Med.* 2012;67:42–49 doi: 10.1002/mrm.22970.
5. Bush A, Borzage M, Detterich J, et al. Empirical model of human blood transverse relaxation at 3 T improves MRI T2 oximetry. *Magn. Reson. Med.* 2017;77:2364–2371 doi: 10.1002/mrm.26311.
6. Jain V, Langham MC, Wehrli FW. MRI estimation of global brain oxygen consumption rate. *J. Cereb. Blood Flow Metab.* 2010;30:1598–607 doi: 10.1038/jcbfm.2010.49.